Development of a Model of Elevated Intraocular Pressure in Rats by Gene Transfer of Bone Morphogenetic Protein 2

LaKisha K. Buie, Md.Zahidul Karim, Matthew H. Smith, and Teresa Borrás

Department of Ophthalmology, University of North Carolina School of Medicine, Chapel Hill, North Carolina

Correspondence: Teresa Borrás, Department of Ophthalmology, University of North Carolina School of Medicine, 4109C Neuroscience Research Building, CB 7041, 105 Mason Farm Road, Chapel Hill, NC 27599-7041;
tborras@med.unc.edu.

Submitted: January 13, 2013
Accepted: June 24, 2013

Citation: Buie LK, Karim MZ, Smith MH, Borrás T. Development of a model of elevated intraocular pressure in rats by gene transfer of bone morphogenetic protein 2 (BMP2). *Invest Ophthalmol Vis Sci*. 2013;54:5441–5455. DOI:10.1167/iovs.13-11651

Purpose. To determine whether inducing calcification in the trabecular meshwork results in elevated IOP in living rats. To use this property to create an elevated IOP animal model by gene transfer of bone morphogenetic protein 2 (BMP2).

Methods. Calcification was assessed by alizarin red staining in primary human trabecular meshwork (HTM) cells and alkaline phosphatase (ALP) activity in the angle tissue. Brown Norway (BN) and Wistar rats were intracamerally injected with Ad5BMP2 (OS) and control Ad5.CMV-Null (OD). IOPs were taken twice a week and expressed as mean integral pressures. Morphology was assessed on fixed, paraffin-embedded anterior segments. Retinal ganglion cells (RGCs) were quantified on retrograde and Brn-3a–labeled flat mounts using MetaMorph software.

Results. BMP2-treated cells displayed marked increase in calcification. Trabecular meshwork tissue showed moderate ALP activity at 13 days postinjection. Fifty-four of 55 BN and 15 of 19 Wistar rats displayed significantly elevated IOP. In a representative 29-day experiment, the integral IOP difference between treated and control eyes was 367.7 ± 83 mm Hg-days ($P = 0.007$). Morphological evaluation revealed a well-organized trabecular meshwork tissue, exhibiting denser matrix in the treated eyes. The Ad5BMP2-treated eye showed 34.4% ± 4.8% ($P = 0.00002$) loss of peripheral RGC over controls.

Conclusions. Gene transfer of the calcification inducer *BMP2* gene to the trabecular meshwork induces elevated IOP in living rats without altering the basic structure of the tissue. This strategy generates an elevated IOP model in rats that would be useful for evaluation of glaucoma drugs targeting the outflow pathway.

Keywords: rat, elevated IOP model, trabecular meshwork, adenoviral gene transfer

Elevated IOP remains the major risk factor for the development of glaucoma,[1,2] an irreversible blindness disease of high prevalence worldwide.[3] Elevated IOP is the result of an increased resistance of the trabecular meshwork tissue to aqueous humor outflow. This increased resistance can be caused by a variety of dysfunctional trabecular meshwork cells and mechanisms. Functions such as secretion, phagocytosis, cytoskeletal organization, cell-matrix adhesion, ion channel transport, signal transduction, proteasome activity, and stiffness have all been shown to have a role in, and to affect, outflow facility. It is widely accepted though, that the most common source of an increase in outflow resistance is the disruption of the organization of the trabecular meshwork's extracellular matrix (ECM).[4,5]

Based on previous findings from our laboratory,[6–8] we have proposed that the trabecular meshwork undergoes a pathological calcification process with age[6] and that this calcification is more prevalent in glaucoma specimens than in age-matched controls.[7] The undergoing calcification observed in the trabecular meshwork has many similarities with the calcification exhibited by vascular smooth muscle cells (VSMCs) and the formation of atherosclerotic plaques,[9,10] and appears to be regulated by many of the same procalcific and anticalcific genes.[6,7] Thus, the trabecular meshwork highly expresses Matrix Gla (MGP) protein,[11] an inhibitor of calcification that is responsible for protecting calcification of other soft tissues, such as cartilage, VSMCs, and kidney.[9,12] After its synthesis, the MGP protein experiences a vitamin K–dependent posttranslational modification that results in binding of calcium and a conformational change. It has been shown in various cell types (including the trabecular meshwork) that the mechanism by which MGP inhibits calcification is through the binding of this activated form of the protein to bone morphogenetic protein 2 (BMP2), a potent inducer of bone formation.[13–16]

BMP2 belongs to the superfamily of TGFβ proteins. BMP2 by itself has the full potential to initiate bone formation and to induce the differentiation of multipotent mesenchymal progenitor cells to the osteogenic lineage.[14,17] Similarly, BMP2 induces osteogenic-like characteristics in primary human trabecular meshwork (HTM) cells in vitro.[6] Overexpression of the *BMP2* gene carried by an adenoviral vector in primary HTM cells induces alkaline phosphatase (ALP) activity,[6] an enzyme that produces a local increase of free phosphate and contributes to the formation of calcium phosphate precipitates (hydroxyapatite crystals), which are part of the mineralization process. Formation of the first crystal occurs in the matrix vesicles, 100-nm particles that originate by budding of the cellular membrane and then are released into the extracellular space. In the ECM, the matrix vesicles release the crystal that gets deposited on collagen fibrils and continues to grow using the first hydroxyapatite crystal as a template.[18,19]

Putting all these findings together, we hypothesized that overexpression of an inducer of the calcification gene in the trabecular meshwork tissue would be sufficient to elevate IOP. We further reasoned that if elevated IOP were to occur upon induction of trabecular meshwork calcification, the gene transfer system could be used to generate feasible hypertensive animal models without damaging (e.g., scarring or laser treatment) the trabecular meshwork. The immediate advantages of such a system would include the possibility of using the model for assaying trabecular meshwork conventional and gene therapy pharmaceuticals, and the relative ease of creating elevated IOP/glaucoma animal models using this approach.

There are currently a variety of animal models available for the study of different types of glaucoma (reviewed recently in Bouhenni et al.[20]). Not all of them are adequate for the evaluation of glaucoma drugs. The current genetic models usually develop elevated IOP at a late onset and some of them lack synchronicity.[21–24] The spontaneous primary open angle glaucoma (POAG) beagle dog model develops high IOP at 1 to 2 years of age[21] and the recombinants MYOC mutant Y423H and collagen type 1–deficient mice exhibit high IOP between 5 and 6 months.[22,25] The Vav-deficient mice, which lack two of the Rho GTPases activating factors, exhibit earlier high IOP onset and late closure of the angle,[24] and the systemic pigment dispersion mice (DBA/2J) exhibit secondary IOP elevation.[23] The steroid-induced models in small and large animals respond well to glaucoma drugs and most require administration two to three times per day for the elevated IOP[26,27] or the implant of osmotic mini pumps.[28] The recently studied polystyrene microbead injection model in mice is very promising, with early-onset IOP, retinal ganglion cell (RGC) damaging, and open angles.[29,30] Another series of models are designed to study the effect of the high IOP insult on RGCs and optic nerve degeneration, but these are not suitable for trabecular meshwork studies. Of these, the most widely used, the Morrison model,[31] injects saline through the episcleral veins, induces sclerosis, and irreversibly damages the functional architecture of the trabecular meshwork. The Sharma model[32] induces elevated IOP by cauterizing two to three episcleral veins and destroys the trabecular meshwork's ability to regulate IOP.

In this study, we used a gene transfer strategy to generate an ocular hypertensive model in a living animal that does not damage the trabecular meshwork. We selected the inducer of calcification gene *BMP2* and delivered it intracamerally to rats in an adenoviral vector. Physiological, molecular, and morphological characterization of the model indicated its potential use for testing conventional and gene therapy pharmaceuticals targeting the trabecular meshwork.

Materials and Methods

Primary Culture of HTM Cells

Nonglaucomatous eyes from human donors were obtained within 40 hours of death from national eye banks (Lions Eye Bank of Oregon, Portland, OR; National Disease Research Interchange, Philadelphia, PA; The North Carolina Eye Bank, Winston-Salem, NC) after signed consent of the patients' families. One cell line, HTM-109, was generated from the residual cornea rim after a surgical corneal transplant at the North Carolina Eye Clinic. All procedures were in accordance with the tenets of the Declaration of Helsinki. For isolation of HTM cells, the trabecular meshwork from both eyes of a single individual were isolated from surrounding tissue by making incisions both anterior and posterior to the meshwork and removing it with forceps. The tissue was then cut into small pieces and treated with 1 mg/mL collagenase type IV (Worthington, Lakewood, NJ), as described.[33] Experiments in this study were performed with cell lines HTM-41, -47, -49, and -109 (ages 15–39 years old). Cells were used at passages four to six. These outflow pathway cultures comprise all cell types involved in maintaining resistance to flow. That includes cells from the three distinct regions of the trabecular meshwork plus cells lining the Schlemm's canal (SC). Because most of the cells in these cultures come from the trabecular meshwork, they are commonly referred to as "trabecular meshwork cells."

Viral Vectors and Infection of HTM Cells

The original Ad5BMP2 adenoviral vector was generously donated by E.A. Olmstead-Davis (Baylor College of Medicine) and has been described.[34] It contains the full-coding cDNA of the human *BMP2* gene driven by the cytomegalovirus (CMV) promoter. The Ad5.CMV-Null adenovirus was purchased from Qbiogene (Montreal, Canada). The Ad5 virus AdhMGP contains the *MGP*s cDNA driven by the CMV promoter and was generated in our laboratory.[6] The self-complementary adeno-associated viral vector scAAV2.GFP contains the enhanced GFP driven by human CMV promoter.[35]

All high-titer adenovirus stocks were prepared by propagation in QBI-HEK 293A cells and purification by double binding CsCl density centrifugation as described.[36,37] The collected viral CsCl band was desalted with NAP-5 columns (GE Healthcare, Piscataway, NJ) equilibrated with virus vehicle (0.01 M Tris, pH 7.4, 1 mM MgCl2, 10% glycerol), aliquoted, and saved at −80°C. Viral particles (VPs) were titered either by measurement of its DNA optical density at 260 nm using the formula 1 μg of DNA = 2.2×10^{10} particles (early lots), or as viral genomes (vg)/mL by real-time PCR using the Ad5 custom-designed fluorescent *Taq*Man primers/probe (University of North Carolina pathology core facility). The Ad5 probe uses the hexon gene Ad5 specific primers forward: 5′TAG CAT TTG CCT TTA CGC CA3′ and reverse: 5′CGT TTC TAA GCA TGG CCT CA (gene bank accession number AY601635, nts 20,673–20,692, and 20,749–20,730, respectively, based on Vora et al.[38]) and a *Taq*Man probe with a FAM fluorophore attached to the 5′ and a tetramethylrhodamine (TAMRA) quencher at the 3′ (*Fam*-5′CCC CAT GGC CCA CAA CAC CGC3′-*Tamra*). For this, viral DNA was extracted from 10 μL purified virus (DNeasy tissue kit; QIAGEN, Valencia, CA), and amplification reactions were set in triplicate. A standard curve was generated by amplifying known copy numbers of a laboratory Ad plasmid standard and plotting them against their threshold cycle (C_T) values. The number of vg was then determined by correlation of the C_T values of the viral DNA to the standard curve. Viral infectivity (infectious units [IFU]/mL) was measured with a rapid titer kit (AdenoX; Clontech, Mountain View, CA), as described.[37] One of the Ad5BMP2 lots was grown at the University of North Carolina Vector Core facility. Viral lots used in these studies had concentrations between 5.5×10^{12} and 1.7×10^{10} VP/mL.

For viral infection, HTM cells at the indicated passages were grown to 70% to 80% confluency, washed twice with PBS, and exposed to Ad5BMP2 at multiplicity of infection (moi) ranging from 5000 to 8000 VPs per cell for 1 hour in 1 mL serum-free medium. After exposure to the virus, serum was added to 2% fetal bovine serum (FBS) and incubated overnight, and full medium containing 10% FBS was added the next day. Incubation continued at 37°C, and fresh medium was replaced every 48 hours.

Alizarin Red Staining and ALP Determination

Infected and uninfected cells at 3 to 5 days postinfection were washed with PBS and fixed in cold 100% methanol at −20°C for

10 minutes. They were then washed with ice-cold distilled water twice and exposed to fresh 1.5% alizarin red (pH 4.2; Sigma-Aldrich, St. Louis, MO) for 5 minutes (red-orange shows positive staining). Subsequently, cells were gently washed with ice-cold distilled water at least three times and photographed with a microscope-mounted digital camera (DP70; Olympus, Center Valley, PA).

ALP activity was determined from tissue extracts and normalized to genomic DNA. Rat anterior segment tissue strips from Ad5BMP2- and Ad5.CMV-Null–treated eyes containing the trabecular meshwork were dissected from the angle area and stored at −80°C. Tissues were thawed, homogenized, and lysed in a sterile glass micro tissue grinder (Micro-All-Glass-Tissue Grinder; Kimble-Chase, Vineland, NJ) with 200 μL PBS. After two more freezing/thawing cycles, tissue homogenates were briefly sonicated and centrifuged. Supernatants were collected and saved at −80°C for the measurement of endogenous ALP and DNA for normalization. ALP was measured using a fluorescence substrate system (AttoPhos AP; Promega, Madison, WI) that does not contain an endogenous ALP inhibitor. Triplicates of 5-μL aliquots were adjusted to 100 μL with PBS and incubated with 100 μL AttoPhos substrate at room temperature in a black microlon 96-well plate (Greiner Bio-One, Monroe, NC) in the dark. A parallel set of incubations was conducted with different dilutions (from 5 ng to 100 ng) of a purified ALP enzyme (Clontech) to generate a standard curve. Controls containing PBS aliquots without enzyme were run in parallel. Fluorometric values were usually read after 20 minutes incubation time in a FLUOstar fluorescence plate reader (BMG Lab Technologies, Durham, NC) with a 430-nm excitation and 555-nm emission filters. ALP accepted readings were from values falling inside the standard curve. For the DNA relative quantity, 30 μL from the treated and control tissue extract supernatants were purified by applying them directly to a QIAquick Gel extraction kit column (QIAGEN) and elution with 30 μL of manufacturer's buffer according to recommendations; 1 μL from treated and untreated samples was then amplified and hybridized to an 18S *Taq*Man Probe (Hs99999901_s1) by real-time PCR (Applied Biosystems [ABI], Carlsbad, CA). Relative quantities of treated versus control DNAs were expressed on fold changes (FCs) and calculated by using the formula $2^{-\Delta C_T}$ (ΔC_T is the difference of the cycles at threshold between treated and control). ALP fluorescence values of treated and control samples were finally obtained by subtracting the ALP value from PBS controls and normalized by the FC of their DNA.

Experimental Animals

All animal procedures were approved by the Institutional Animal Care and Use Committee at the University of North Carolina and were conducted in accordance with the tenets of the Declaration of Helsinki and the ARVO statement on the Use of Animals in Ophthalmic Research. Rat strains were either male brown Norway (BN) (300–400 g) retired breeders or male Wistar (100–150 g) and were purchased from Charles River Laboratories (Wilmington, MA). All animals were housed in standard 12-hour cycle lighting with food and water provided ad libitum.

Intraocular Administration of Recombinant Viral Vectors

After a brief isoflurane inhalation, each rat was anesthetized by intraperitoneal injection of a ketamine/xylazine/acepromazine (Butler Schein, Columbus, OH) cocktail to achieve concentrations of 50 mg/kg (ketamine), 5 mg/kg (xylazine), and 1 mg/kg (acepromazine), respectively. While resting on its side, the rat was placed under a surgical microscope (Wild Heerbrugg M5A stereo microscope; Adlon Instruments, St. Louis, MO) with the head propped up in a holder and eyes directed upward. The corneas were anesthetized with one drop of 0.5% tetracaine (Bausch & Lomb, Tampa, FL). For the intracameral vector delivery, a 30-gauge needle was inserted through the superior cornea at the limbus with the bevel up, to gently reach the center of the anterior chamber. The needle device consisted of the tip of a 30-gauge needle, broken at the middle, connected to one end of intramedic-polyethylene tubing (PE-10; BD/Clay Adams, Franklin Lakes, NJ). The remaining half of the needle, plus the hub, was attached at the other end of the tubing and then connected to a dispenser (Gilmont micrometer syringe; Thermo Fisher Scientific, Waltham, MA). The tubing was partially filled with a colored glycerol driving solution to allow aspiration of 4 to 5 μL of the viral sample. Inside the tubing, the driving solution was kept separated by 3 to 4 cm from the sample at all times. When the needle was inside the anterior chamber, the sample was delivered by the assistant over 30 seconds and fluid entry monitored by direct visualization through the operating microscope (Wild Heerbrugg M5A stereo microscope; Adlon Instruments). The needle was left in place for 1 to 2 minutes and withdrawn gradually to minimize leaking. Topical antibiotic ointment (neomycin 3.5 mg/g, polymyxin B 10,000 U/g, and bacitracin 400 U/g; Akorn, Lake Forest, IL) was placed on the eyes, and the animals were returned to their cages, resting on absorbent paper for recovery.

RNA Extraction, Reverse Transcription, and Real-Time PCR

HTM cells either uninfected or Ad5BMP2-infected, were scraped from 3-cm tissue culture dishes with 350 μL guanidine thiocyanate buffer (RLT; QIAGEN) at 3 days postinfection. Total RNA was extracted by loading the solution onto a column (QIAshredder; QIAGEN) and continued by the use of a kit with on-column RNase-free DNase digestion (RNeasy Mini kit; QIAGEN) in accordance with the manufacturer's recommendations. Purified RNA was eluted in 30 μL RNase-free water and concentration measured with a spectrophotometer (NanoDrop ND-100; Thermo Fisher Scientific). Recoveries were between 13.4 and 18.6 μg per dish.

Rat angle tissue strips containing the trabecular meshwork were excised from globes immersed for 1 week in RNA*later* (Ambion, Austin, TX). Globes were dissected at the equator and the posterior segment discarded. Anterior segments were cleaned of the iris and lens, the ciliary body was carefully folded back, and two parallel cuts were made at both sides of the trabecular meshwork using an Optimal microsurgery blade (Wilson Ophthalmics, Mustang, OK). The tissue strip was placed in a sterile glass micro-tissue grinder (Kimble-Kontes), homogenized with 350 μL guanidine thiocyanate buffer, and loaded onto a column (QIAshredder; QIAGEN). Treated and untreated eyes from two rats were pooled and RNA extraction was continued as indicated above for the human cells. Recoveries were between 1.1 and 2.4 μg RNA per extraction.

Reverse transcription (RT) reactions were conducted in a 25-μL total volume of proprietary RT buffer containing random primers, dNTPs, and 62.5 U of enzyme with RNase inhibitor (MultiScribe MuLV RT; High Capacity cDNA kit; ABI), according to manufacturer's recommendations (25°C for 10 minutes, 37°C for 2 hours, 85°C for 5 minutes). The total amount of RNA used in each of the RTs was 1 μg for the human cells and 0.46 μg for the rat angle tissue.

Fluorescently labeled *Taq*Man probe/primer sets for human *BMP2*, collagen type I alpha1 (*COL1A1*), osteoglycin (*OGN*),

Investigative Ophthalmology & Visual Science

runt-related transcription factor 2 (*RUNX2*), osteocalcin (*BGLAP*), bone sialoprotein 2 (*IBSP*), and 18S, as well as those for rat *COL1A1*, *RUNX2*, *BGLAP*, *IBSP*, and *MGP* were purchased from the *Taq*Man Gene Expression Assays collection (ABI). The human *BMP2* (Hs00154192_m1) corresponded to sequences from exons 2 and 3, the human *COL1A1* (Hs00164004_m1) and *BGLAP* (Hs01587814_g1) corresponded to sequences from exons 1 and 2, the human *OGN* (Hs00247901_m1) corresponded to sequences from exons 3 and 4, the human *RUNX2* (Hs001047973_m1) corresponded to sequences from exons 5 and 6, and the human *IBSP* (Hs00173720_m1) corresponded to sequences from exons 4 and 5. The rat *COL1A1, RUNX2*, *BGLAP*, *IBSP*, and *MGP* (Rn001463848_m1, Rn01512298_m1, Rn00566386_g1, Rn00561414_m1, Rn00563463_m1) probes corresponded to sequences from exons 1 and 1, 2 and 3, 3 and 4, 4 and 5, 1 and 2, respectively; the 18S RNA probe corresponded to sequences surrounding position nucleotide 609 (Hs99999901_s1). Reactions were performed in triplicate 20-μL aliquots using *Taq*Man Universal PCR Master mix No AmpErase UNG (ABI), run on an ABI 7500 Real-Time PCR System, and analyzed by 7500 System SDS v.2.0.4 software (ABI). Experiments were repeated at least twice. Relative quantification (RQ) values between treated and untreated samples were expressed in FC and calculated by the formula $2^{-\Delta\Delta C_T}$, where C_T is the cycle at threshold and ΔC_T is C_T of the assayed gene minus C_T of the endogenous control (18S). $\Delta\Delta C_T$ is the ΔC_T of the normalized assayed gene in the treated sample minus the ΔC_T of the same gene in the untreated one (calibrator). Because of the high abundance of the 18S ribosomal RNA used as the endogenous control, and in order to get a linear amplification, RT reactions from treated and untreated samples were diluted 10^4 times prior to their hybridization to the 18S *Taq*Man probe.

Measurement of IOP

IOPs were measured unmasked in sedated rats once or twice a week. At the beginning of the study, IOPs were recorded with a calibrated handheld tonometer (Tonopen XL; Mentor, Norwell, MA). Midway through the study, IOPs were measured by the use of the rebound tonometer. The rebound tonometer used for approximately half of the rat groups was one of the prototypes developed at Mount Sinai School of Medicine (New York, NY) and generously provided to us by Thomas Mittag and John Danias.[39,40] The IOP of the remaining groups was measured using the TonoLab (Colonial Medical Supply, Franconia, NH) equipped with a foot pedal. The rats were lightly anesthetized with the described isoflurane/intraperitoneal cocktail at half-dose and with an eye drop of 0.5% tetracaine. To take IOP measurements, the rats were positioned with the visual axis horizontal to the probes. For the tonopen, IOPs were obtained as the average of 10 consecutive measurements for each eye. For the prototype rebound tonometer, the probe was held at a distance between 1 and 4 mm and five consecutive readings (arbitrary units that correlate to IOP) were obtained by pressing the foot pedal connected to the probe power supply. Only mean values with an SD (expressed as percentage of the mean) less than 5% were accepted. This tonometer was calibrated on rats at the same ages as those used in the experiments (before and 3.5 months after injection) by ex vivo cannulation and manometric readings as described.[40] IOP-correlated values were obtained by creating a logarithmic calibration curve with the tonometer and manometric values, and then obtaining the a and b constant values in the formula $Y = aLn(X) - b$, where X is the correlated IOP and Y is the tonometer's measurement. The calibration curves had correlation coefficients of 0.98 and 0.96, respectively. For the Tonolab, IOP measurements were conducted following manufacturer's recommendations. Integral IOP (cumulative pressure received by each rat on the entire duration of the experiment) was calculated using the Area Under the Curve (AUC) tool of the GraphPad Prism 5 software (GraphPad Software, Inc., La Jolla CA).

Histology and Fluorescence Histochemistry

Rats' eyes were enucleated immediately after euthanization and immersed either in fresh 4% paraformaldehyde (PFA) in PBS for 30 minutes or in RNA*later* (Ambion) for 5 to 7 days at 4°C. For histological evaluations, the eyes were subsequently dissected at the equator, their lens removed, and wedge-shaped specimens containing the anterior chamber angle region with the trabecular meshwork were postfixed for morphology or GFP fluorescence. To assess morphology, wedges were immersed in 4% PFA/2.5% glutaraldehyde at room temperature for at least 24 hours followed by immersion in 0.1 M cacodylic acid, pH 7.35, overnight. Specimens were then rinsed in distilled water for 10 minutes and transferred to 70% ethanol for delivery to the University of North Carolina Histology Core for paraffin embedding. Meridional 5-μm sections were mounted on microscope slides (Superfrost Plus; Thermo Fisher Scientific) and stained with hematoxylin and eosin. To evaluate GFP fluorescence, tissue wedges were postimmersed in fresh 4% PFA from 4 to 18 hours, then consecutively washed in 10% sucrose (6 hours) and 30% sucrose (overnight) and frozen in optimal cutting temperature medium (Tissue-Tek; Sakura Finetek, Torrance, CA) in liquid nitrogen. Meridional 10-μm sections were mounted on Superfrost Plus microscope slides (Thermo Fisher Scientific) with Fluoromount G (SouthernBiotech, Birmingham, AL) and GFP visualized with a fluorescence microscope (model IX71; Olympus). Images were captured with a digital camera (DP70; Olympus) and accompanying software. Digital images were arranged with image-analysis software (Photoshop CS; Adobe Photoshop, Mountain View, CA). Quantification of fluorescence intensities in treated and control images was carried out using MetaMorph for Olympus digital imaging software (Olympus). In each experiment, exposure for nonsaturated conditions was first determined using the brightest tissue section and then using the obtained exposure value in all specimens of the same experiment. Total intensity of the area of the trabecular meshwork was measured in the green channel by tracing the region in the brightest image and transferring it to the comparison images using the transfer region and region statistics tools of the program.

RGCs Retrograde Labeling and Brn-3a Immunohistochemistry

Loss of RGCs was assessed in labeled flat mounts by two procedures: retrograde labeling and immunocytochemistry. For the retrograde labeling, rats were deeply anesthetized by intramuscular injections of a ketamine/xylazine cocktail to a dose of 70 mg/kg ketamine and 30 mg/kg xylazine. Rats were then immobilized on a stereotaxic apparatus (KOPF, Tujunga, CA), their head fur shaved, and exposed skin infiltrated with 1% bupivacaine (Hospira, Inc., Lake Forest, IL). A 1- to 2-cm incision was made to expose the dorsal surface of the skull and sutures. With the help of a caliper, microinjection points were drawn on the skull 6 mm posterior to bregma and 2.0 mm lateral to the sagittal suture. Openings were made through the skull at the marked sites to expose the superior colliculus using a Micro Drill system (World Precision Instruments, Sarasota, FL). A 5-μL Hamilton 65RN syringe,

Investigative Ophthalmology & Visual Science

equipped with a 2-inch 30G RN NDL point 4 needle (Hamilton, Reno, NV) was loaded with a 3% Dil dye solution (Molecular Probes/Life Technologies, Carlsbad, CA) (dissolved in dimethyl sulfoxide–ethanol 1:1) and placed in the stereotaxic frame. Using the stereotaxic's micromanipulator (KOPF), the needle was lowered 4.5 mm to deliver 1.5 μL of the tracer. The needle was kept in place for 10 minutes, slowly withdrawn, antibiotic ointment (erythromycin, 5 mg/g; E. Fougera & Co., Melville, NY) applied and the skin incision sutured with 2-0 silk, nonabsorbable suture (Oasis, Mettawa, IL). Rats were placed on top of deltaphase isothermal pads at 37°C (Braintree Scientific, Braintree, MA) for recovery. Seven days after tracer labeling, rats' eyes were enucleated immediately after euthanization and immersed in fresh 4% PFA for 1 hour with a corneal puncture. Eyes were then opened at the limbus, lens and ciliary body removed, and retinal cups rinsed with PBS and treated with 20 μg/mL hyaluronidase (Sigma-Aldrich) for 30 minutes at room temperature. Consecutively, retinal cups were postfixed for 30 minutes and washed in PBS overnight. The next morning, retinas were dissected from the underlying sclera/choroid, flattened by four radial cuts, mounted vitreal side up on Superfrost Plus slides (Thermo Fisher Scientific), and coverslipped with a drop of antifade mounting medium containing 0.1 mg/mL *p*-phenylenediamine (Sigma-Aldrich) in 90% glycerol/PBS, pH 8.0 (PPD). Images were taken in an Olympus XI71 fluorescence microscope equipped with an Olympus DP70 digital camera and software. For each retina, images were taken from 20, ×20 fields (0.394 mm^2) located at 0.5 mm from the periphery (two per quadrant). Automated cells counts in each field were obtained on the gray scale mode using MetaMorph software for Olympus (Olympus) and using the same threshold value. For each individual retina, the total count of surviving RGC neurons was obtained by averaging the eight counts for each retina. Results are expressed in percentage of RGC loss in the Ad5BMP2-treated eyes versus the Ad5.CMV-Null-control. The two groups in each experiment were analyzed for differences using the Student's paired *t*-test.

For the immunohistochemistry procedure, rats were either immersed in 4% PFA for 1 hour as indicated above, or perfused through the heart using a gravity system (In Vivo Perfusion System, 70 cm high; AutoMate Scientific, San Francisco, CA) following the manufacturer's recommendations. Briefly, rats were deeply anesthetized with intraperitoneal injection of 100 to 400 mg/kg of euthasol (Butler Schein) and their chest cavities opened. A 20G × 3/4-inch scalp vein set (EXEL International, Los Angeles, CA) was inserted into the left ventricle and approximately 150 mL 0.9% NaCl was perfused through the circulatory system after making a slit on the right atrium to allow perfusion. Perfusion continued with 400 to 600 mL 4% PFA made in 0.1 M phosphate buffer pH 7.2 until the rat's body was stiff. Eyes were then immediately enucleated and treated like above for flat mounting on Superfrost Plus slides (Thermo Fisher Scientific). Subsequently, a hydrophobic ring was drawn around the retina using a Liquid Blocker super pap-pen (Newcomer Supply, Middleton, WI), retinas were rinsed with PBS/0.5% Triton X-100 and permeabilized at −80°C for 15 minutes. Alternatively, the nonperfused, hyaluronidased/postfixed retinas were separated from the sclera/choroid, kept in solution in 24 wells for all immunohistochemistry steps, and flat mounted after the last wash. For this, after thawing them at room temperature, in-well retinas were washed and blocked with 2% donkey serum/PBS/0.5% Triton X-100 for 1 hour. Retinas were then incubated with goat antihuman Brn-3a antibody (1:550, sc-31984; Santa Cruz Biotechnologies, Santa Cruz, CA) overnight followed by an additional 2 hours with donkey antigoat Alexa Fluor 568 (1:550; Molecular Probes/Life Technologies). All antibody solutions were made in 2% donkey serum/PBS/0.5% Triton X-100, and three washes (PBS/0.5% Triton X-100) were performed between incubation steps. Slides with retinal flat mounts were briefly dried on the slide warmer and coverslipped with a drop of Fluoromount G (SouthernBiotech). Images were taken with either a Zeiss LSM 510 Meta confocal (Carl Zeiss Group, Oberkochen, Germany) or an Olympus XI71 microscope equipped with its own digital camera software (LSM 510 for the confocal and DP70 for the Olympus). For each retina, images were taken from eight, ×20 fields (0.212 and 0.394 mm^2, respectively) at half field from the periphery. Quantification was subsequently performed as indicated above.

Conventional Glaucoma Drugs

The prostaglandin formulation used was 0.01% lumigan (Allergan, Inc., Irvine, CA). A 50-μL drop of the formulation was administered twice a day to the OD of conscious rat by holding them down gently at the bottom of the cage. Control eyes received PBS drops from a clean 50-μL dispenser eye drop bottle or no drops.

Statistical Analysis

Average values are expressed as mean ± SE. The significance of experimental changes was analyzed using Student's *t*-test as either paired or unpaired data. For the calculation of *P* values, all technical replicates from all biological replicates were used. A value of 0.05 was chosen as the level of significance. The power of the experiments was determined using the GraphPad StatMate2 software (GraphPad Software, Inc.).

Results

Overexpression of BMP2 Induces Calcification in Primary HTM Cells

We have previously shown[6] that infection of primary HTM cells with a recombinant adenovirus carrying the *BMP2* transgene (Ad5BMP2)[34] increased the activity of ALP, an established marker of early osteogenic differentiation.[41,42] Here we examined the morphology of the HTM cells by staining them with alizarin red, also a widely used calcification marker. BMP2-infected cells from all cell lines examined in this study ($n = 4$) showed marked calcification morphology when stained with alizarin red. The cells from infected dishes began to retract 2 days postinfection and aggregated in elongated structures that stained positive for calcification (Fig. 1A1). Young, noninfected cells showed no aggregates, and exhibited normal cell morphology (Fig. 1A2). The characteristic aggregated cell organization had the appearance of a small tissue explant and was more pronounced at specific conditions such as later postinfection times and in HTM cell lines that have been aged in culture for more than 4 weeks (Fig. 1A3). Old, HTM noninfected cells also calcified, but formed the more typical calcification round nodules (Fig. 1A4) previously described for VSMCs.[6]

Extracted RNAs from treated and untreated cells were analyzed for induction of expression of calcification gene markers by *Taq*Man PCR. When normalized to 18S cDNA, transgene human *BMP2* cDNA levels were increased 22,904 ± 4398-fold ($P = 0.007$) in the infected cells over those treated with vehicle, confirming high delivery and expression of the *BMP2* transgene. This *BMP2* overexpression induced human

Investigative Ophthalmology & Visual Science

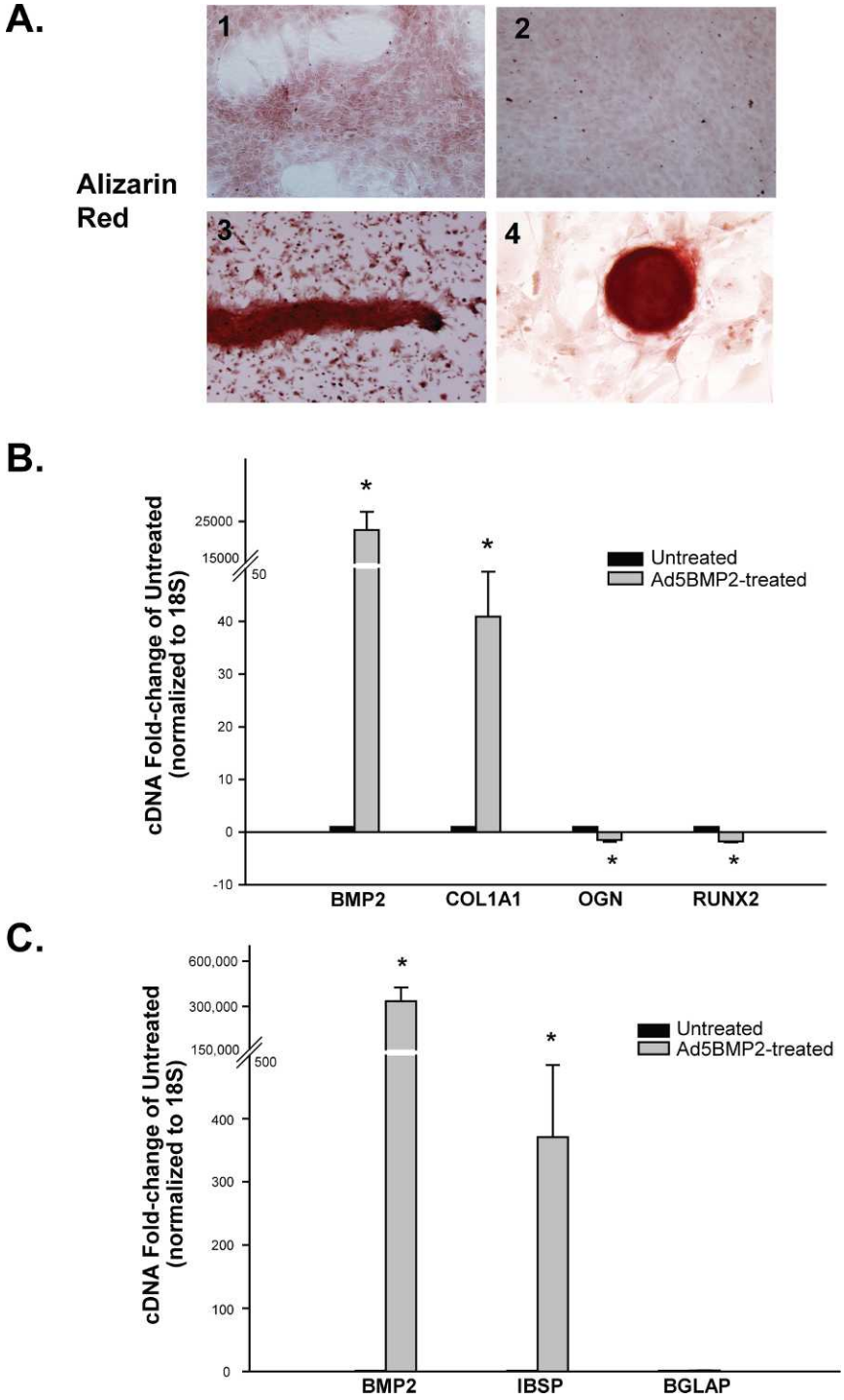

Figure 1. Effect of overexpressing *BMP2* in primary HTM cells. Cells at passage 5 and 70% to 80% confluency were infected with Ad5BMP2 at moi between 5000 and 8000 VP/cell and harvested 3 to 5 days postinfection. (**A**) Cells stained with alizarin red. (*1*) corresponds to a representative infected well at 3 days postinfection, whereas (*2*) represents a parallel uninfected dish. A second HTM cell line was aged in culture for 2 months, infected with Ad5BMP2, and stained at 5 days postinfection (*3*). (*4*) represents a parallel dish of 2 months aged in culture uninfected cells. (**B, C**) *Taq*Man analysis of the RNA extracted from HTM-infected and untreated controls at 3 days postinfection, in two different cell lines. Results are expressed in FC of the infected versus the untreated and normalized to 18S. Human *Taq*Man probes were *BMP2*, *COL1A1*, *OGN*, *RUNX2*, *IBSP*, *BGLAP*, human 18S. $^*P \leq 0.05$. Overexpression of *BMP2* induced calcification in HTM cells as well as expression of *COL1A1* and *IBSP* markers.

collagen type 1 (*COL1A1*) 41 ± 8.6-fold ($P = 0.01$), while genes for *OGN* and transcription factor *RUNX2* were slightly reduced (−1.5 ± 0.37-fold, $P = 0.002$, and −1.74 ± 0.22-fold, $P = 0.0002$, respectively) (Fig. 1B). The expression of additional calcification markers integrin-binding protein *IBSP* and *BGLAP* were also assayed in a different experiment. In this experiment, where *BMP2* was induced 334,191 ± 91,654-fold ($P = 0.02$), expression of *BGLAP* was not changed (1.3 ± 0.21-fold, $P = 0.18$), while that of *IBSP* was induced 371 ± 114-fold ($P = 0.03$) (Fig. 1C).

Single Intracameral Injection of Ad5BMP2 Delivers Human *BMP2* mRNA to the Cells of the Rat Angle

To first test the positive delivery of the transgene to the rat's angle, four BN rats were injected with 4 to 5 μL of 1.3×10^{12} VP/mL stocks of Ad5BMP2 (OS) and Ad5.CMV-Null (OD) viral vectors. Thirteen days after injection, RNA was harvested from two of the rat's pooled angle tissues and assayed in triplicate for the presence of human *BMP2* (transgene) by *Taq*Man PCR. The human *BMP2* gene expression was undetected in the OD control eyes and thus assigned a C_T of 40 for calculations. When normalized to 18S, expression of human *BMP2* cDNA in the Ad5BMP2-treated eye (OS) versus that of Ad5.CMV-Null-treated controls (OD) was 112 ± 19-fold ($P = 0.03$). In a similar trend as in the human cells, overexpression of human BMP2 protein in the angle of the living rat induced the expression of the osteogenic differentiation marker *COL1A1* 2.9 ± 0.6-fold over that of the control eye ($P = 0.04$) but at this time period, it did not change the expression of *RUNX2* (1.03 ± 0.4, $P = 0.9$). At these levels of human BMP2 overexpression, the calcification markers *IBSP* and *BGLAP* were not induced (0.75 ± 0.3, $P = 0.5$ and 0.84 ± 0.2, $P = 0.4$, respectively) (Fig. 2A).

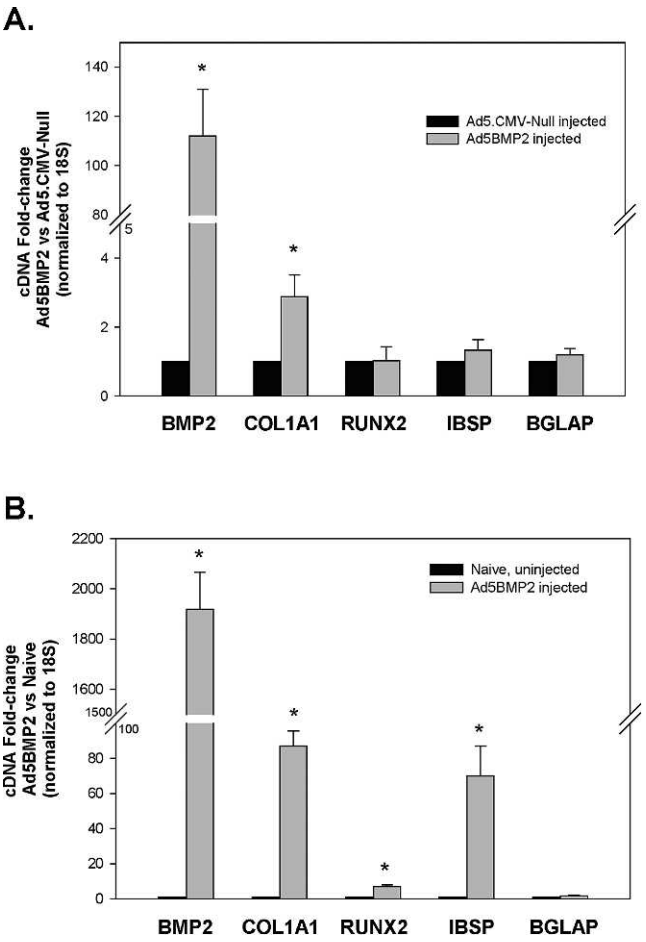

Figure 2. Delivery of human *BMP2* cDNA to the living rat iridocorneal angle by Ad5BMP2 intracameral injection: its effect on expression of calcification genes. Tissue strips from the angle region containing the trabecular meshwork were dissected at 12 to 13 days postinjection and their RNA extracted for *Taq*Man analyses. Results are expressed in FC of the Ad5BMP2-injected rats versus controls and normalized to 18S. (**A**) OS eyes of BN rats ($n = 4$) were injected with 4×10^9 VP of Ad5BMP2 and compared with their OD receiving the same VPs of Ad5.CMV-Null. (**B**) OS eyes from Wistar rats ($n = 4$) were injected with 2×10^{10} VP of Ad5BMP2 and compared with OD and OS of Wistar Naïve rats ($n = 2$). *Taq*Man reactions were performed in triplicate, each from 2 to 4 independent RT reactions. *Taq*Man probes were human *BMP2*, rat *COL1A1*, rat *RUNX2*, rat *IBSP*, rat *BGLAP*, human 18S. $^*P \leq 0.05$. Transgene human *BMP2* was efficiently delivered to the rat iridocorneal angle. At higher concentrations, overexpression of human *BMP2* induced rat *COL1A1*, *RUNX2*, and *IBSP* calcification markers in the living rat.

The experiment was repeated two additional times using two rats' pooled angle tissues from a different group of Wistar rats injected with 4 to 5 μL from a different 5.5×10^{12} VP/mL Ad5BMP2 viral stock versus two pooled tissues of naïve rats. RNA was harvested at 12 days postinjection. Each time, three independent cDNA RT reactions were assayed in triplicate by *Taq*Man PCR using the same probes indicated above normalized by 18S. Results were very similar, but FC changes were more pronounced, most likely due to the use of a higher-titer viral stock. Although human *BMP2* expression was undetected in the naïve rats (assigned a C_T value of 40 for calculations), its expression exhibited an increase of 1918 ± 148-fold ($P = 2 \times 10^{-9}$) in the Ad5BMP2-injected eyes. At these high levels of *BMP2* overexpression, *COL1A1* was induced 86.9 ± 8.6-fold ($P = 2 \times 10^{-7}$) over the naïve eye, *RUNX2* was increased 7.0 ± 0.9-fold ($P = 0.00003$) and *IBSP* was induced 70 ± 17-fold ($P = 0.0003$). The *BGLAP* gene remained, as above, uninduced (1.8 ± 0.4, $P = 0.07$) (Fig. 2B).

Together, these results indicate that calcification markers are induced by a dose-dependent overexpression of *BMP2* and suggest that calcification could be one of the causes of the elevated IOP observed in the Ad5BMP2-injected eyes. Induction of some of the markers, such as bone sialoprotein 2 (*IBSP*), seems to appear only when the *BMP2* cDNA levels are higher.

Single Intracameral Injection of Ad5BMP2 Induces Sustained Elevated IOP in Rats

A total of 74 rats (55 BN and 19 Wistar) were injected in the anterior chamber of one eye with 8×10^7 to 2.7×10^{10} VP of Ad5BMP2 (treated) in different studies. The contralateral eye was similarly injected with the same range of VP of Ad5.CMV-Null (control). Elevated IOP of the treated versus the control was observed in 54 of the 55 BN and in 15 of the 19 Wistar rats. The pressures were elevated at approximately 7 days postinjection and sustained for up to 6 to 7 weeks. To maximize transgene delivery, maximum intracameral injection volumes (4–5 μL) were always used and the extent of elevated IOP seemed to be affected by the number of VP injected and, to some extent, by the rat strain. BN rats experienced a higher IOP elevation in the treated eye than Wistar rats, with a TonoLab (Colonial Medical Supply) mean difference between IOP values at 4 weeks ([treated − baseline] − [control − baseline]) of 25.2 ± 2.4 ($n = 15$, $P = 1 \times 10^{-10}$). In the original experiments, Wistar rats exhibit a lower but highly significant elevation at the same time period with ΔIOP values of 3.5 ± 0.6 ($n = 13$, $P = 1 \times 10^{-7}$). However, when a higher concentration viral stock was used, the Wistar rats' ΔIOP increased and the difference between the two strains diminished (see the Initial Responsiveness to Conventional and Gene Therapy Glaucoma Drugs section).

Figure 3 shows two representative experimental groups of BN rats where IOP values were obtained using either the tonopen (Figs. 3A, 3C) or the TonoLab (Colonial Medical Supply) (Figs. 3B, 3D). In the tonopen experiment (Fig. 3A), absolute IOP values for the Ad5.CMV-Null control and Ad5BMP2-treated eyes were plotted at baseline, 7, 16, 28, 36, 42, and 48 days ($n = 10$ rats). The mean absolute IOPs of the Ad5BMP2-injected eyes were 24.4 ± 0.3 mm Hg at baseline and 42.3 ± 1.9 mm Hg at 48 days postinjection ($n = 10$, $P = 0.000005$), whereas those of the Ad5.CMV-Null–injected eyes

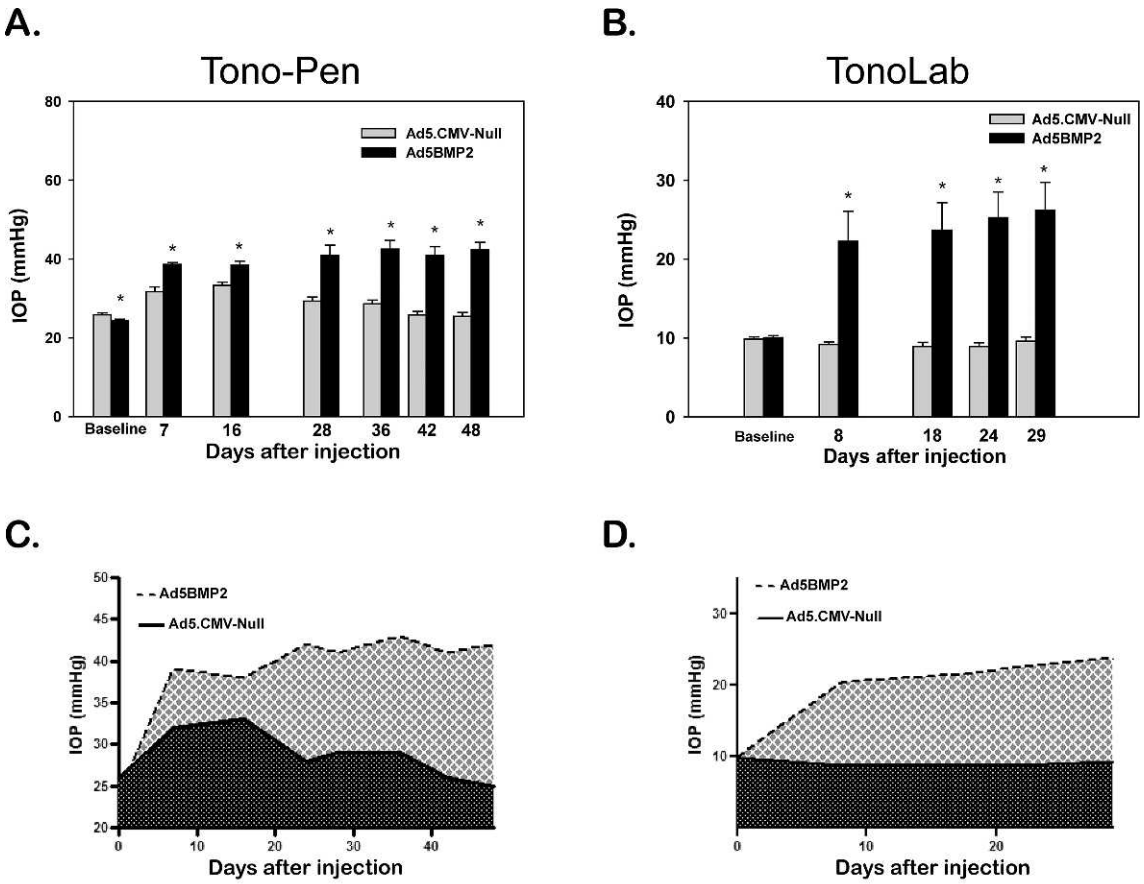

E.

Exp	Treatment	Duration (days)	Peak IOP Difference [(BMP2-basl)-(Null-basl)] mmHg	Integral IOP (mmHg-days)	Integral IOP Difference (mmHg-days)
Tonopen	Ad5BMP2 Ad5.CMV-Null	48 (n=10) 48 (n=10)	18.4 ± 1.7	1886.6 ± 58.3 1403.2 ± 31.5	483.4 ± 61.6
TonoLab	Ad5BMP2 Ad5.CMV-Null	29 (n=6) 29 (n=6)	20.2 ± 4.3	634.0 ± 86.8 266.3 ± 8.6	367.7 ± 83.3

Figure 3. Rat elevated IOP induced by overexpression of human *BMP2* cDNA. Two representative BN rat groups were injected with 5×10^9 to 9×10^7 VP Ad5BMP2 (OS) and 7×10^9 to 9×10^8 VP Ad5.CMV-Null (OD), respectively. IOP was measured using a tonopen (**A**, **C**) or a TonoLab rebound tonometer (**B**, **D**). (**A**) IOP absolute values of treated and control eyes from the tonopen group ($n = 10$) during 48 hours after injection. Mean baseline IOP of all eyes was 25.3 ± 0.3 mm Hg. (**B**) IOP absolute values of treated and control eyes from the TonoLab group ($n = 6$) during 29 days after injection. Mean baseline IOP of all eyes was 9.9 ± 0.1 mm Hg. $^*P \leq 0.05$ at the last time points (**A**, **B**). (**C**, **D**) AUC plots of the mean IOPs of treated (*broken line*) and control eyes (*continuous line*) from the tonopen (**C**) and TonoLab (**D**) groups. The integral IOP differences are depicted in *gray*. (**E**) Summary table of the numeric values of measurements and calculations of IOP differences between treated and controls in both groups, $P \leq 0.007$. Delivery and overexpression of the human BMP2 transgene to the iridocorneal of the living rat induces significant elevation of IOP when compared with controls.

were 25.9 ± 0.4 mm Hg at baseline and 25.4 ± 1.0, also at 48 days ($n = 10$, $P = 0.70$). Thus, at the last time period of 48 days, the mean ΔIOP elevation from baseline was 17.9 ± 1.9 mm Hg in the Ad5BMP2-injected eyes and −0.5 ± 1.1 mm Hg for the contralateral control ($n = 10$, $P = 0.000005$ and $P = 0.70$, respectively). Considering the whole study period, the animal with the highest ΔIOP from baseline (peak ΔIOP baseline) in the treated eye had an IOP elevation of 33.0 mm Hg at 24 days (full range of all animals 12.0 to 33.0 mm Hg). For the mean IOP difference between treated and contralateral control eyes (peak IOP difference), the highest value was 18.4 ± 1.7 mm Hg ($n = 10$, $P = 0.000002$) at 48 days. The animal with the highest IOP difference between its treated and contralateral control eyes had an IOP elevation of 33.0 mm Hg at 24 days (full range of all animals 16.0–33.0 mm Hg). The mean integral IOP (defined as the mean of the cumulative IOP that each animal received for the duration of the experiment) was 1886.6 ± 58.3 mm Hg-days for the Ad5BMP2-injected eyes and 1403.0 ± 31.5 mm Hg-days for the Ad5.CMV-Null–injected eyes, which results in an integral IOP difference of 483.6 ±

Investigative Ophthalmology & Visual Science

61.6 mm Hg-days ($n = 10$, $P = 0.00003$). The highest integral IOP difference in a single animal was 758 mm Hg-days.

In the TonoLab (Colonial Medical Supply) experiment (Fig. 3B), absolute IOP values for the Ad5.CMV-Null control and Ad5BMP2-treated eyes were plotted at baseline and 8, 18, 24, and 29 days ($n = 6$ rats). Of the seven rats injected, one did not show elevated pressure and was excluded from the study. The mean absolute IOPs of the Ad5BMP2-injected eyes were 10.0 ± 0.3 mm Hg at baseline and 26.2 ± 3.6 mm Hg at 29 days postinjection ($n = 6$, $P = 0.005$), whereas those of the Ad5.CMV-Null–injected eyes were 9.9 ± 0.3 mm Hg at baseline and 9.6 ± 0.5 at 29 days ($n = 6$, $P = 0.67$). Thus, at the same time period, the mean ΔIOP elevation from baseline was 16.1 ± 3.4 mm Hg in the Ad5BMP2-injected eyes and –0.3 ± 0.6 mm Hg for the contralateral control ($n = 6$, $P = 0.005$ and $P = 0.67$, respectively). Considering the whole study period, the animal with the highest ΔIOP from baseline (peak ΔIOP baseline) in the treated eye had an IOP elevation of 27.2 mm Hg at 29 days (full range of all animals 11.2 to 27.2 mm Hg). For the IOP difference between treated and contralateral control eyes, the highest value (peak IOP difference) was 20.2 ± 4.3 mm Hg ($n = 6$, $P = 0.006$) at 29 days. The animal with the highest IOP difference between its treated and contralateral control eyes had an IOP elevation of 29.3 mm Hg at 29 days (full range of all animals at all time periods 10.5 to 29.3 mm Hg). The mean integral IOP was 634.0 ± 86.8 mm Hg-days for the Ad5BMP2-injected eyes and 266.3 ± 8.6 mm Hg-days for the Ad5.CMV-Null–injected eyes, which results in an integral IOP difference of 367.7 ± 83.3 mm Hg-days ($n = 6$, $P = 0.007$). The highest integral IOP difference in a single animal was 626.8 mm Hg-days.

Clinical Observations and Trabecular Meshwork Morphology of Rats Injected With Ad5BMP2

As we reported before, intracameral injections of recombinant adenoviruses are well tolerated by rats.[35] After intracameral injections of Ad5BMP2 and Ad5.CMV-Null viruses there were no clinical signs of inflammatory reaction, redness, or tearing. However, approximately 30% of the eyes from the BN rats injected with Ad5BMP2 exhibited an enlarged globe and a moderate corneal opacity. The opacity correlated with the enlarged globe that, in turn, correlated with those individual rats showing the highest increase in IOP values of the group. Such opacity was not observed in the eyes of Wistar rats.

The morphology of the trabecular meshwork injected with Ad5BMP2 was assessed versus that of the contralateral eye injected with Ad5.CMV-Null. Although some variation among individual rats could be observed, in all cases the trabecular meshwork was well preserved and the angle was open. Representative images from different experiments with Wistar and BN rats are shown in Figure 4 and Supplementary Figure S1, respectively. Most morphologies of the Ad5BMP2-injected

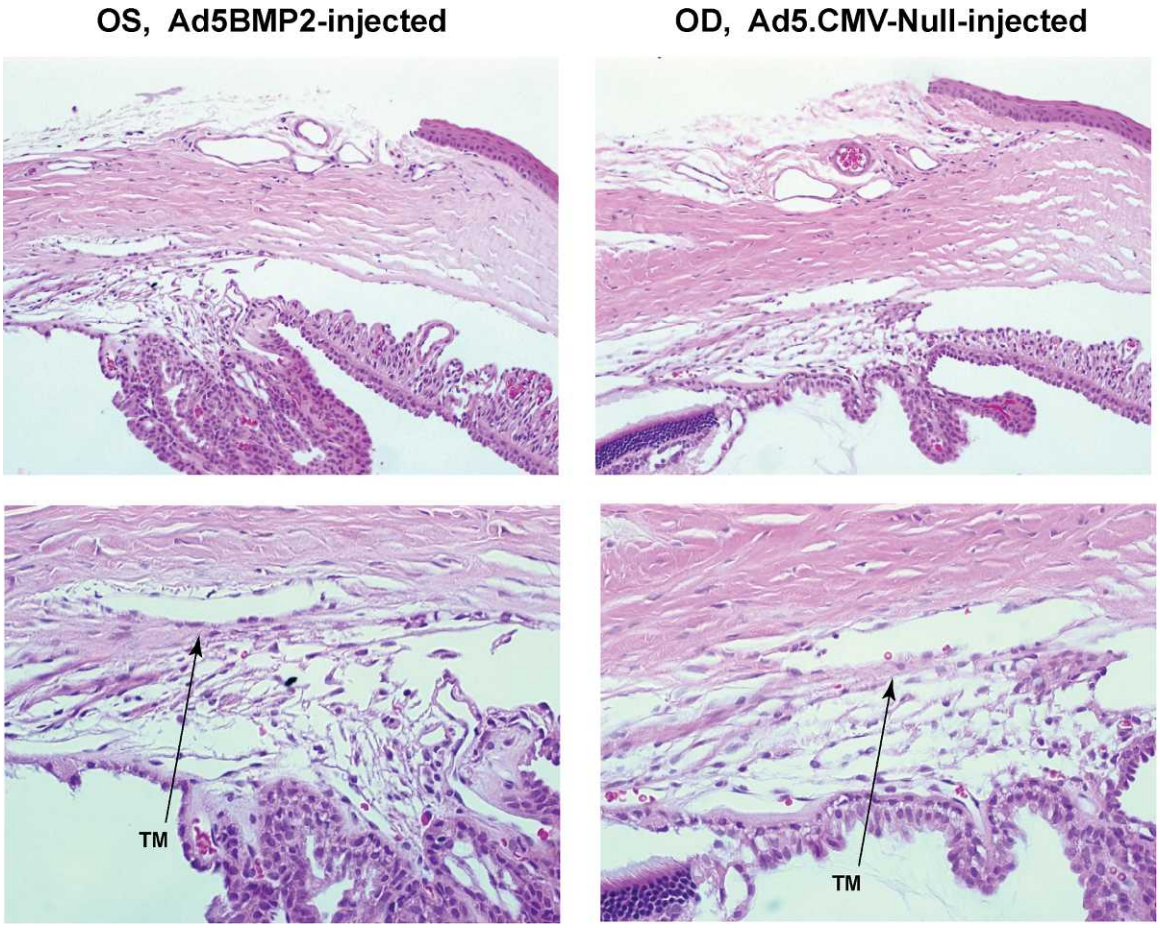

Figure 4. Morphology of the rat trabecular meshwork after gene transfer of *BMP2*. Representative images of the eye angle region from a group of Wistar rats injected with 5×10^9 VP of Ad5BMP2 (OS, *left*) and 1×10^9 Ad5.CMV-Null (OD, *right*) and killed at 77 days postinjections. Anterior segment wedges were fixed in 4% paraformaldehyde/2.5% glutaraldehyde, embedded in paraffin, and 5-μm sections stained with hematoxylin and eosin. Original magnification: ×100 (*top*), ×200 (*bottom*). TM, trabecular meshwork; SC, Schlemm's canal. Ad5BMP2-treated eye shows an open angle and a well-conserved trabecular meshwork structure with a denser ECM than the contralateral Ad5.CMV-Null control.

Investigative Ophthalmology & Visual Science

eye could be easily distinguished from the Ad5.CMV-Null contralateral eye. Although both eyes showed an intact trabecular meshwork structure, the region underneath the SC appeared to be more dense in the BMP2-overexpressing rats, with less empty spaces in between the beams, as if it they were filled with more ECM (Fig. 4 and Supplementary Fig. S1, left panels). At this light microscopy resolution, we could not observe a strong correlation between a given morphology and the levels of elevated IOP. Rats experiencing a moderate elevation in IOP also showed an increased density, which often did not appear to be much different from the density observed in the higher IOP rats. Although not physically counted, the number of trabecular meshwork cells observed in both treated and control eyes appeared to be maintained (Fig. 4, Supplementary Fig. S1).

Evaluation of RGCs

Because prolonged elevated IOP induces damage to the RGC layer, we tested whether the pressure induced by BMP2 overexpression affected the survival of these cells in two groups of BN rats at 29 to 28 days post–viral injection. Evaluation of RGCs was performed by different methods. In the first group, four rats from the TonoLab (Colonial Medical Supply) experiment (Fig. 3) were injected with 3% DiI into the superior colliculus at 29 days post-Ad5BMP2 injections. Three of four rats showed significant RGC loss (Fig. 5A). In the peripheral region (0.5 mm for the periphery), the percent average RGC loss in the *BMP2*-treated eyes versus the Null-treated eyes was 34.3% ± 4.8% ($P = 0.00002$).

In the second BN group ($n = 9$ rats, 28 days), RGCs were labeled using Brn-3a immunohistochemistry rather than the more invasive superior colliculus dye injection. Sixteen retina flat mounts from eight of the nine rats were suitable for counting. Of the 16, 7 retinas from Ad5BMP2-injected eyes experienced a significant peripheral RGC loss when compared with the 7 from their contralateral eyes injected with Ad5.CMV-Null. The average RGC loss in the *BMP2*-treated eyes versus the Null-treated was 31.0% ± 4.8% ($n = 7$, $P = 0.0006$) (Fig. 5B). In a supporting Brn-3a immunohistochemistry experiment with Wistar rats, where the IOP elevation of Ad5BMP2-injected eyes was smaller due to a lower titer viral

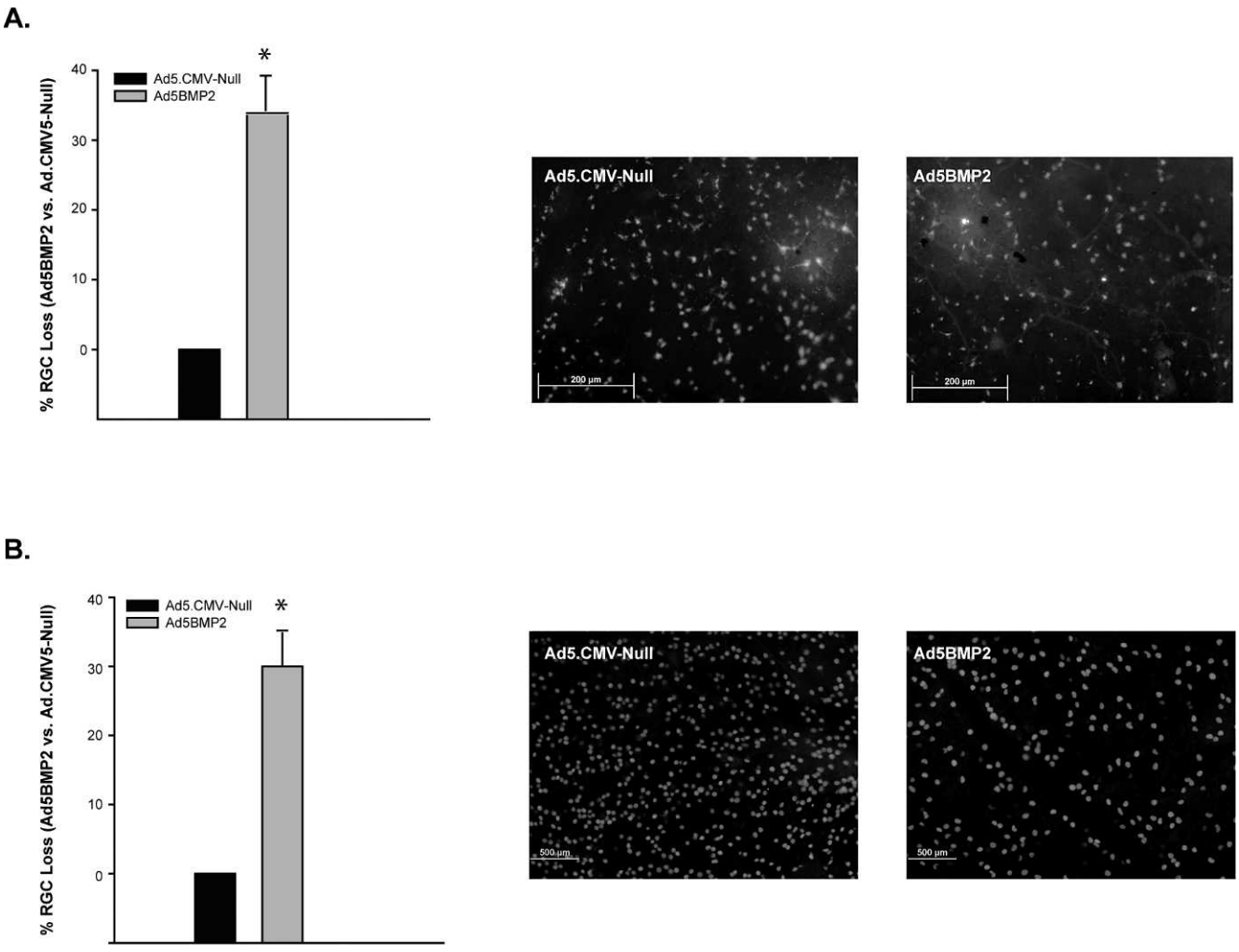

Figure 5. Effect of BMP2-induced elevated IOP on RGC survival. (**A**) BN rats ($n = 3$) injected with 7×10^7 VP of Ad5BMP2 (OS) and 7×10^8 VP of Ad5.CMV-Null (OD) were retrograde labeled with 3% Dil solution at 29 days postinjection. (**B**) Retinas of BN rats ($n = 7$) injected with 2.7×10^{10} VP of Ad5BMP2 (OS) and 7×10^8 VP of Ad5.CMV-Null (OD) were flat mounted and stained with Brn-3a at 28 days postinjection. *Left*: percentage of DiI- (**A**) or Brn-3a-labeled (**B**) RGC cell loss in the treated eyes normalized to untreated. *Right*: representative fluorescence photomicrographs of treated and untreated flat-mounted retinas taken from the peripheral retina. The number of positive cells was obtained from eight peripheral fields per each flat-mounted retina using MetaMorph software. The number of positive RGC cells was significantly reduced in the elevated IOP-BMP2 treated eyes. $^*P \leq 0.006$.

Investigative Ophthalmology & Visual Science

stock, we saw a smaller, albeit significant, RGC loss in the periphery of the retina 16.3% ± 1.5% ($P = 0.02$) ($n = 3$). In this group, the average IOP cumulative difference between the Ad5BMP2- and Ad5.CMV-Null–treated eyes was 133 mm Hg-days, whereas the cumulative difference in the BN experiments above were 367 and 729 mm Hg-days, respectively.

Altogether, these results indicate that at 4 weeks, the elevated IOP induced by overexpression of BMP2 is not only a result of TonoLab (Colonial Medical Supply) readings but it has, as expected, a physiological effect on the RGC.

Alkaline Phosphatase Activity on the Rat Angle Tissue

The levels of the calcification marker ALP were measured in two groups of BN rats at 23 and 28 days postinjection, respectively. In the first group ($n = 5$), one eye was injected with 2×10^{10} VP of Ad5BMP2, while the contralateral was left uninjected. Elevated IOP was observed at 7 days in all injected eyes and averaged an increase over baseline of 37 ± 5.5 mm Hg at 23 days, when the experiment was terminated. Angle tissue strips were homogenized for the extraction of ALP and DNA, as indicated in the Methods section. After normalizing for the amount of genomic DNA in each tissue strip, we found that the levels of ALP in the Ad5BMP2-injected versus uninjected tissue varied, and were elevated in only two of the five rats. The values ranged between an increased 189% ALP in the eye of one viral-injected rat ($P = 0.00002$) to a reduction of 56.6% in another rat ($P = 0.00008$). In the second group of rats ($n = 5$), the IOP of the Ad5BMP2-injected eyes had an increase over baseline of 31.1 ± 1.1 mm Hg at 28 days, when the rats were killed. Although the variation trend continued, the higher levels of normalized ALP in the BMP2 eyes were observed in a greater proportion of rats. Thus, of the five, ALP was high in three rats (77.7% ± 7.4%, $P = 0.0005$), low in one of them (3.4%, $P = 0.32$), and reduced 41.3% in the fifth rat ($P = 0.0007$).

The lower levels of ALP in the eyes of some rats injected with Ad5BMP2 were unexpected and would appear to contradict the established effect of the bone inducer BMP2. At this time, we interpret this finding as perhaps due to the potential presence of high concentration of the BMP2-inhibitor MGP in the trabecular meshwork tissue, which would induce a counteracting effect and lead to a minimal, undetected calcification. Indeed, the measured relative levels of rat *MGP* cDNA in the angle strips of naïve rats showed a *MGP* expression of 174.9 ± 40.6-fold when compared with the low-expressing rat *BGLAP* gene ($P = 0.002$). The undetected calcification level seen in several rats was nevertheless sufficient to induce elevated IOP. To this effect, a recent study shows that the proximity between MGP and BMP2 proteins plays a role in ossification.[43] One could speculate that the lack of control of which trabecular meshwork regions are transduced by Ad5BMP2 after intracameral injection could result in different distribution that would be more or less affected by the presence of MGP.

Initial Responsiveness to Conventional and Gene Therapy Glaucoma Drugs

To initiate validating the model as a potential tool for evaluating conventional and/or gene drugs, we performed two types of experiments. For the testing of conventional drugs, we used two Wistar rat groups. In one group ($n = 6$), four rats were injected with Ad5BMP2 in both eyes, treated with the drug in one eye and left the contralateral eyes untreated to serve as controls. The remaining two rats were injected with Ad5BMP2 in the OS and left untreated, while their OD was uninjected and treated with PBS drops. At 13 days postinjection, the ODs of the first four rats were treated with one drop of lumigan 0.01% twice a day for 3.5 consecutive days, while their OS remained untreated. The average IOP of the lumigan-treated eyes before Ad5BMP2 injections was 9.0 ± 0.4 mm Hg and showed an increase of 19.6 ± 3.8 mm Hg at 9 days postinjection ($n = 4$, $P = 0.01$). After lumigan administration (measured 2 hours post–last administration, total 16 days post–viral injection) the IOP showed an increase from baseline of only 8.9 ± 4.6 mm Hg, which corresponds to a reduction of 55.1% ($P = 0.07$) from IOP values before the treatment. Six days after lumigan withdrawal, the IOP showed an increase from baseline of 12.4 ± 3.7 mm Hg, indicating a wearing off of the drug effect. For the untreated controls, the OS Ad5BMP2-injected, non–lumigan-treated eyes ($n = 6$) had an average IOP of 8.9 ± 0.2 mm Hg before viral injections and experienced an increase from baseline of 15.8 ± 2.5 mm Hg (9 days postinjection, $P = 0.001$), 12.6 ± 1.5 mm Hg (16 days, $P = 0.0005$), and 15.5 ± 1.8 mm Hg (22 days, $P = 0.0004$). The two additional OD eyes that had been uninjected and treated with PBS drops for 3.5 days showed average IOPs of 9.6 ± 0.4 mm Hg at baseline, 9.3 ± 0.3 mm Hg at 9 days, 8.5 ± 0.2 mm Hg at 16 days, and 9.8 ± 1.5 mm Hg at 21 days.

Following a similar design, in the second group ($n = 5$), four rats were injected with Ad5BMP2 in both eyes. Then, the OD was treated with the drug in OD while the contralateral untreated OS served as a control. As above, an additional rat was injected with Ad5BMP2 in only one eye (OS) while the OD received PBS drops to assess contralateral effect. The average IOP of the OD lumigan-treated group before Ad5BMP2 injections was 9.0 ± 0.3 mm Hg and showed an increase from baseline of 30.0 ± 1.3 mm Hg at 7 days postinjection ($n = 4$, $P = 0.0002$). Lumigan administration started at 8 days postinjection and IOP was measured 2 hours post–last administration at day 12, when the experiment was terminated. After the lumigan treatment, IOP values showed an increase from baseline of 3.8 ± 2.0 mm Hg, corresponding to a reduction of 87.3% ($P = 0.0008$) from IOP values before the treatment (Fig. 6A). The OS, Ad5BMP2-injected, non–lumigan-treated eyes ($n = 5$) had IOPs of 9.4 ± 0.3 mm Hg (baseline) and exhibited increases from baseline of 29 ± 0.9 mm Hg (7 days, $P = 0.000006$) and 31.4 ± 1.1 mm Hg (12 days, $P = 0.00001$) (Fig. 6B). An additional virus uninjected/untreated eye had IOPs of 10.5 mm Hg at baseline, 10.7 mm Hg at 7 days and 10.0 mm Hg at 12 days (all uninjected/untreated eyes in Fig. 6C). Altogether, these results suggest that the BMP2-induced elevation IOP model holds good promise for the evaluation of conventional trabecular meshwork drugs.

Initial experiments with gene therapy drugs showed that pretreatment of the Ad5BMP2-injected eye with an adenovirus of the same serotype 6 days before the high IOP induction precluded the Ad5BMP2-induced IOP elevation ($n = 8$, half of them pretreated with Ad5.CMV-Null and half with AdhMGP,[6] both serotype 5). Using a reporter gene, we then observed that postinjection of the Ad5 serotype with a scAAV.GFP serotype 2, at 29 days allowed expression of the reporter gene ($n = 4$). At 1 week post–reporter injection, the quantification of fluorescence in a traced trabecular meshwork area of 111,268 pixels minus background showed an average of 15.8 fluorescence intensity units per pixel (FIU/pix). In contrast, postinjection with a virus of the same serotype, Ad5.GFP, showed an average of 6.2 FIU/pix under the same conditions ($n = 3$). In a different experiment, postinjection of the same serotype at 7 days showed 5.2 FIU/pix (traced area 161,777 pixels minus background) ($n = 2$). However, coinjection of the Ad5 reporter with Ad5BMP2 allowed expression of the *GFP* transgene (36.0 FIU/pix on a trabecular meshwork–traced area 166,980 pixels

Investigative Ophthalmology & Visual Science

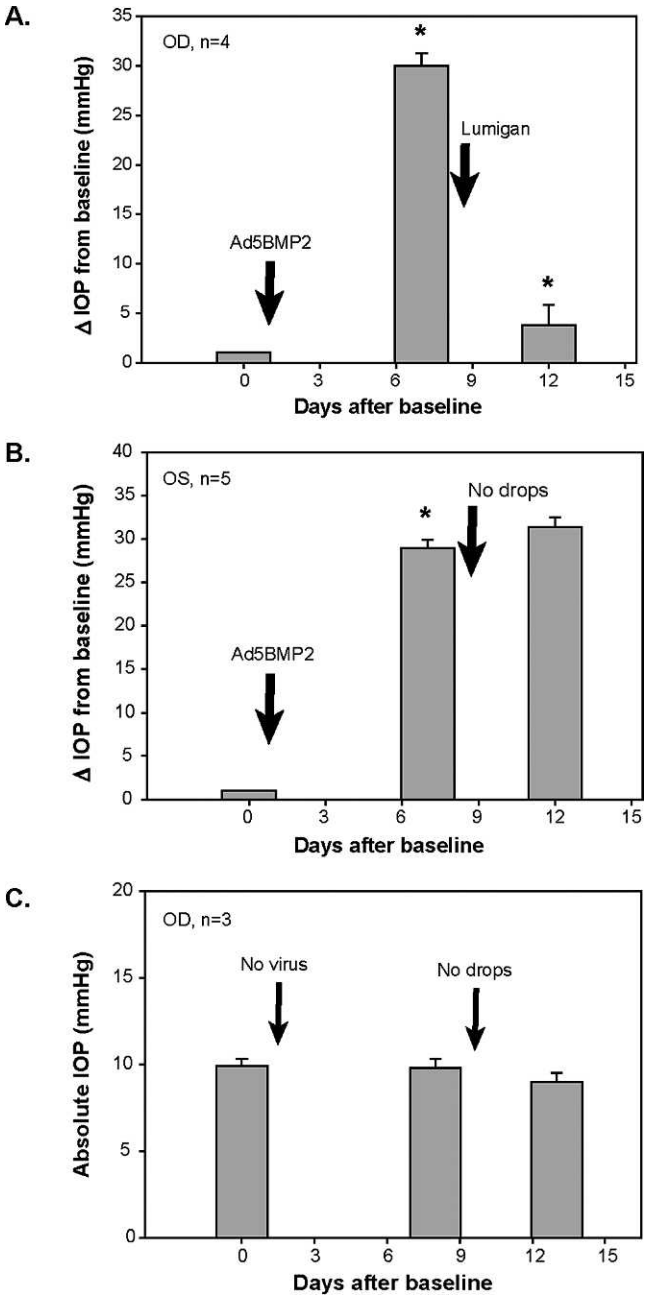

FIGURE 6. Representative experiment of the evaluation of the BMP2 model with a prostaglandin-derived glaucoma drug. Eyes of Wistar rats were injected with 2×10^{10} Ad5BMP2 VP ($n = 9$) or left uninjected ($n = 3$). At 8 days postinjection, eyes were (**A**) treated twice a day for 3.5 days with one drop of 0.01% lumigan ($n = 4$), or (**B**) left untreated (no drops, $n = 5$). (**C**) Uninjected eyes treated with PBS ($n = 3$). IPO measurements are expressed as ΔIOP from baseline (**A**, **B**) or absolute values (**C**). *$P \leq 0.05$. Rats with BMP2-induced elevated IOP exhibit a significant IOP reduction on treatment with a conventional glaucoma drug.

minus background). Fluorescence quantification of the reporter transgene without previous Ad5BMP2 or Ad5.CMV-Null injections was not available. These results indicate that serotypes would play an important role when assaying viral gene therapy drugs in this model, and that the gene therapy drugs will work best on viral IOP models generated by a different serotype.

DISCUSSION

Convenient, small animal models to evaluate trabecular meshwork drugs for the treatment of hypertension and glaucoma are scarce.[20] Most of them consist of genetically modified mice that develop elevated IOP at 5 to 8 months of age, often in an asynchronous mode, which makes it difficult to study drug evaluation. One of the more promising recent advances is the microbead model, in which beads, a bead/viscoelastic combination, or paramagnetic polystyrene microspheres are injected into the anterior chamber of mice and rats to clog the outflow pathway.[29,30,44,45] Since our laboratory has developed transgene delivery to the trabecular meshwork using viral vectors,[35–37,46] we reasoned that an additional animal model of elevated IOP could be generated by gene transfer to the outflow tissue. We further hypothesized that overexpression of a secreted gene in the trabecular meshwork that would contribute to the formation of a denser ECM, would most likely result in elevated IOP. In our search for a candidate ECM-IOP inducer gene we came to rely on our previous findings that revealed the presence of an ongoing calcification process in the trabecular meshwork.[6] For this study, we selected *BMP2*, one of the most potent calcification inducer genes.[47] We found that a single intracameral dose of the Ad5BMP2 vector to the trabecular meshwork of living rats was sufficient to induce elevation of IOP.

In contrast to most existing models, the elevation of IOP had a rapid and uniform onset and could be observed at 7 days postinjection. In addition, the elevated IOP was maintained for at least 4 to 6 weeks after injection of the virus, which provides an extended period of time for the assay of glaucoma drugs. As expected, the extent of elevated IOP is dependent of the number of VP injected, thus the titer and age of the viral stock need to be taken into account. Rats seem to be an ideal animal for this IOP model. Their anterior segment morphology is clearly defined and exhibits a well-formed SC. Of the two rat species studied, BN had a somewhat higher response than the Wistar rats and both strains tolerate adenovirus intraocular injection without developing a clinical inflammatory reaction. BN rats had already been identified as a preferred small animal to conduct IOP/RGC studies due to their gentle nature and protruding eyes, which makes conducting intraocular injections and taking IOP measurement relatively easy.[31] The only drawback we found in this BMP2 model was that some of the BN rats exhibiting higher delta pressures developed a moderate corneal opacity, a secondary effect that would preclude an intraocular evaluation by current optical coherence tomography technology in this rat strain. Except for that exclusion, all other evaluation parameters, such as frequent IOP measurements and molecular, histological, immunohistochemistry, and RGC survival end points, can be performed adequately and together can provide a complete assessment of the assaying drug. The corneal opacity was not observed in the Wistar rats.

It is important to note that this rat model was generated using a human *BMP2* cDNA. Although the identification of the transgene would be more difficult because of hybridization probes cross-reacting with the endogenous gene, it is possible that the IOP effect would be further improved by using the homologous gene.

An important characteristic of this model is that the architecture and cellular organization of the trabecular meshwork is preserved. Morphology images showed that the angle remains open with an apparent increase of ECM between the layers of the trabecular meshwork tissue. As a consequence, this model could be used to evaluate glaucoma drugs that target the trabecular meshwork. To this effect, our first experiments using lumigan drops were very encouraging and

showed an IOP reduction of 55% to 87% after instillation of eye drops twice a day for 3.5 days.

The mechanism of action for the increased IOP in this rat model is not yet fully determined. BMP2 is a potent inducer of calcification/bone formation and recombinant BMP2 administrations have been approved by the Food and Drug Administration for the treatment of bone fracture repair. Previously we have shown that HTM cells transduced with the same Ad5BMP2 vector and overexpressing human *BMP2* had increased levels of the calcification marker ALP, and that this effect was reversed by co-transduction with *MGP*.[6] Here we show that a similar transduction in these cells induces dramatic morphological calcification changes. The cells of the dish retracted from each other and aggregated forming structures that stained deeply with alizarin red. Under these conditions, the calcification markers' transcripts, collagen type 1 and bone sialoprotein, assayed by real-time PCR, were significantly upregulated, whereas those encoding for *OGN*, *RUNX2*, and *BGLAP* were not. This indicates that the morphological calcification observed in the trabecular meshwork cells is influenced more by the higher induction of COL1A1 and IBSP levels, and that in these cells calcification can occur without an increased presence of OGN, transcription factor RUNX2, or BGLAP. COL1A1 is an integral component of the calcified matrix vesicles,[8] as well as a key component of the extracellular scaffold of the trabecular meshwork. IBSP binds to collagen and is a major structural protein of the bone matrix. Under noninduced conditions, IBSP is barely detected in the trabecular meshwork which is perhaps the reason why its new presence provokes the calcification changes.

In the trabecular meshwork of the tissue of the living rat, the increased levels of the calcification marker ALP varied with the individual rats. A potential explanation for this result could be that the living trabecular meshwork tissue expresses high levels of MGP, which is considerably downregulated in tissue culture (Borrás T, unpublished observations, 2008). The mechanism of action of the inhibitor of calcification MGP has been shown to be that of binding and sequestering BMP2.[6] As it occurred in the cells, there was a significant induction of *COL1A1* and, at a higher concentration of *BMP2*, there was also significant induction of *IBSP* and to a lesser extent, *RUNX2*. Thus, at this time, we believe that even if the biochemical detection of calcification in the living animal is small, it appears nevertheless to be sufficient to cause an elevation of IOP.

We cannot discard the possibility though, that only a segment of the calcification pathway, or a different alternative pathway elicited by overexpression of BMP2 has a major influence in obstructing the outflow pathway and triggering elevated IOP. For example, it could be possible that the overexpression of *COL1A1*, a key component of the trabecular meshwork ECM found to be elevated in glaucomatous conditions,[48] would by itself elevate IOP. The combination of this with other induced pathways could enhance the outcome. Thus, it has been extensively shown that there is crosstalk between BMP2 and the WNT pathways.[49] The canonical WNT/βcatenin pathway is involved in the commitment of mesenchymal cells to osteoblasts and has been implicated in the pathogenesis of bone diseases.[50] The WNT/βcatenin pathway is crucial for BMP2 to induce bone formation[51] and osteogenic differentiation of dental follicle cells induced by stimulation with BMP2 is suppressed by WNT/βcatenin pathway inhibitors.[49] But in this and other studies, it has been observed that during the osteogenic differentiation, BMP2 also induces expression of the WNT antagonist WIF1, suggesting the presence of a negative feedback mechanism to regulate osteogenesis.[49] Interestingly, the WNT/βcatenin pathway has been shown to be present in the trabecular meshwork and implicated in IOP regulation.[52–55] The WNT antagonist secreted frizzled-related protein 1 (sFRP1) was upregulated by elevated IOP and in glaucomatous samples,[52,53] and its overexpression in the trabecular meshwork by adenoviral delivery reduced outflow facility in perfused human organ cultures. The interaction between the two pathways is complex and it would be interesting to find whether sFRP1 would enhance or abrogate the BMP2 induction of elevated IOP.

The BMP2 elevated IOP model described here responded well to prostaglandin analog–derived drugs. All eight rats tested exhibited an IOP reduction after 3.5 days, twice a day administration of lumigan 0.01%. The prostaglandin drug group's site of action is the uveoscleral and conventional outflow pathways, thus it makes sense that this model, based on the modification of the ECM of the outflow tissue, would respond well to outflow targeting drugs. As a result, our findings place this model on a nice niche for the assay of trabecular meshwork conventional drugs. Experiments to test other types of conventional glaucoma drugs, such as β-blockers, are ongoing. In the present study, we also showed that evaluation of gene therapy drugs in this model is possible, albeit certain considerations are needed. Because the model is based on the injection with a virus of a given serotype, potentially therapeutic transgenes would need to be inserted in viral vectors of a different serotype from the one used to generate the model. Such experiments are in progress and initial results have revealed expression of a serotype 2 reporter following injection of a serotype 5 virus.

In addition to the advantages mentioned above, these gene transfer models provide a new generic, comprehensive platform to develop elevated IOP models, in more than one species and with more than one viral vector. The requirements for their development, in time and cost, are favorable to those of generating transgenic animals. Since our first presentation of this model (Buie LK, et al. *IOVS* 2009;50:ARVO E-Abstract 4841), an IOP model using an adenovirus carrying the active form of *TGFβ2* or connective tissue growth factor *CTNF* has been developed successfully in rats and mice.[56–58] At the current time, no large animal models have been reported. Our first collaborating trials using the same vector in large animals have not yet been successful (Kaufman PL, Weber AJ, Borrás T, unpublished results, 2011) due in great part to the high inflammatory response of large animals to high concentration of adenoviruses.[59] Nevertheless, the same concept could be used by carrying the transgene in a lower inflammatory response vector, such as scAAV or lentiviruses. Adenoviruses have great advantages for rats, including the shorter expression time of the transgene, which could benefit in the evaluation process. Another advantage as usage of viral vectors increases is that many of these viral reagents carrying relative common genes (such as *BMP2*) are available commercially and/or at universities' vector core facilities.

In summary, we are presenting an alternative modality to generate elevated IOP models in living animals by gene transfer. Our first model using a single intracameral administration of the calcification inducer *BMP2* by an Ad5 vector proved to be very efficient in rats. The characteristics of this model, simplicity, short time of onset, uniformity, and, especially, that of keeping an intact trabecular meshwork, provide a unique opportunity for the evaluation of trabecular meshwork-targeted glaucoma drugs. Finally, although mechanisms are not yet fully elucidated, the ocular hypertension observed in these rats on overexpression of *BMP2* suggests that there is an association between induction of calcification and elevation of IOP.

Investigative Ophthalmology & Visual Science

Acknowledgments

The authors thank Brandon Lane for critical reading of the manuscript and helpful comments.

Supported by National Institutes of Health Grants EY11906 (TB) and EY13126 (TB) and by an unrestricted grant from Research to Prevent Blindness to the Department of Ophthalmology at the University of North Carolina at Chapel Hill.

Disclosure: **L.K. Buie**, None; **M.Z. Karim**, None; **M.H. Smith**, None; **T. Borrás**, None

References

1. Anderson DR. Glaucoma: the damage caused by pressure. XLVI Edward Jackson memorial lecture. *Am J Ophthalmol*. 1989;108:485–495.
2. Kass MA, Heuer DK, Higginbotham EJ, et al. The Ocular Hypertension Treatment Study: a randomized trial determines that topical ocular hypotensive medication delays or prevents the onset of primary open-angle glaucoma. *Arch Ophthalmol*. 2002;120:701–713.
3. Sommer A, Tielsch JM, Katz J, et al. Relationship between intraocular pressure and primary open angle glaucoma among white and black Americans. The Baltimore Eye Survey. *Arch Ophthalmol*. 1991;109:1090–1095.
4. Lütjen-Drecoll E, Shimizu T, Rohrbach M, Rohen JW. Quantitative analysis of 'plaque material' in the inner- and outer wall of Schlemm's canal in normal- and glaucomatous eyes. *Exp Eye Res*. 1986;42:443–455.
5. Keller KE, Aga M, Bradley JM, Kelley MJ, Acott TS. Extracellular matrix turnover and outflow resistance. *Exp Eye Res*. 2009;88:676–682.
6. Xue W, Wallin R, Olmsted-Davis EA, Borrás T. Matrix GLA protein function in human trabecular meshwork cells: inhibition of BMP2-induced calcification process. *Invest Ophthalmol Vis Sci*. 2006;47:997–1007.
7. Xue W, Comes N, Borrás T. Presence of an established calcification marker in trabecular meshwork tissue of glaucoma donors. *Invest Ophthalmol Vis Sci*. 2007;48:3184–3194.
8. Borrás T, Comes N. Evidence for a calcification process in the trabecular meshwork. *Exp Eye Res*. 2009;88:738–746.
9. Luo G, Ducy P, McKee MD, et al. Spontaneous calcification of arteries and cartilage in mice lacking matrix GLA protein. *Nature*. 1997;386:78–81.
10. Wallin R, Wajih N, Greenwood GT, Sane DC. Arterial calcification: a review of mechanisms, animal models, and the prospects for therapy. *Med Res Rev*. 2001;21:274–301.
11. Borrás T. What is functional genomics teaching us about intraocular pressure and glaucoma. In: Civan MM, ed. *The Eye's Aqueous Humor*. 2nd ed. San Diego: Elsevier; 2008:323–377.
12. Proudfoot D, Shanahan CM. Molecular mechanisms mediating vascular calcification: role of matrix Gla protein. *Nephrology (Carlton)*. 2006;11:455–461.
13. Böstrom K, Tsao D, Shen S, Wang Y, Demer LL. Matrix GLA protein modulates differentiation induced by bone morphogenetic protein-2 in C3H10T1/2 cells. *J Biol Chem*. 2001;276:14044–14052.
14. Ducy P, Karsenty G. The family of bone morphogenetic proteins. *Kidney Int*. 2000;57:2207–2214.
15. Wallin R, Cain D, Hutson SM, Sane DC, Loeser R. Modulation of the binding of matrix Gla protein (MGP) to bone morphogenetic protein-2 (BMP-2). *Thromb Haemost*. 2000;84:1039–1044.
16. Nakagawa Y, Ikeda K, Akakabe Y, et al. Paracrine osteogenic signals via bone morphogenetic protein-2 accelerate the atherosclerotic intimal calcification in vivo. *Arterioscler Thromb Vasc Biol*. 2010;30:1908–1915.
17. Riley EH, Lane JM, Urist MR, Lyons KM, Lieberman JR. Bone morphogenetic protein-2: biology and applications. *Clin Orthop Relat Res*. 1996;(324):39–46.
18. Anderson HC. Matrix vesicles and calcification. *Curr Rheumatol Rep*. 2003;5:222–226.
19. Yang H, Curinga G, Giachelli CM. Elevated extracellular calcium levels induce smooth muscle cell matrix mineralization in vitro. *Kidney Int*. 2004;66:2293–2299.
20. Bouhenni RA, Dunmire J, Sewell A, Edward DP. Animal models of glaucoma. *J Biomed Biotechnol*. 2012;2012:692609.
21. Gelatt KN, Gum GG, Gwin RM, Bromberg NM, Merideth RE, Samuelson DA. Primary open angle glaucoma: inherited primary open angle glaucoma in the beagle. *Am J Pathol*. 1981;102:292–295.
22. Zode GS, Kuehn MH, Nishimura DY, et al. Reduction of ER stress via a chemical chaperone prevents disease phenotypes in a mouse model of primary open angle glaucoma. *J Clin Invest*. 2011;121:3542–3553.
23. John SW, Smith RS, Savinova OV, et al. Essential iris atrophy, pigment dispersion, and glaucoma in DBA/2J mice. *Invest Ophthalmol Vis Sci*. 1998;39:951–962.
24. Fujikawa K, Iwata T, Inoue K, et al. VAV2 and VAV3 as candidate disease genes for spontaneous glaucoma in mice and humans. *PLoS One*. 2010;5:e9050.
25. Aihara M, Lindsey JD, Weinreb RN. Ocular hypertension in mice with a targeted type I collagen mutation. *Invest Ophthalmol Vis Sci*. 2003;44:1581–1585.
26. Sawaguchi K, Nakamura Y, Nakamura Y, Sakai H, Sawaguchi S. Myocilin gene expression in the trabecular meshwork of rats in a steroid-induced ocular hypertension model. *Ophthalmic Res*. 2005;37:235–242.
27. Gerometta R, Podos SM, Danias J, Candia OA. Steroid-induced ocular hypertension in normal sheep. *Invest Ophthalmol Vis Sci*. 2009;50:669–673.
28. Whitlock NA, McKnight B, Corcoran KN, Rodriguez LA, Rice DS. Increased intraocular pressure in mice treated with dexamethasone. *Invest Ophthalmol Vis Sci*. 2010;51:6496–6503.
29. Sappington RM, Carlson BJ, Crish SD, Calkins DJ. The microbead occlusion model: a paradigm for induced ocular hypertension in rats and mice. *Invest Ophthalmol Vis Sci*. 2010;51:207–216.
30. Yang Q, Cho KS, Chen H, et al. Microbead-induced ocular hypertensive mouse model for screening and testing of aqueous production suppressants for glaucoma. *Invest Ophthalmol Vis Sci*. 2012;53:3733–3741.
31. Morrison JC, Moore CG, Deppmeier LM, Gold BG, Meshul CK, Johnson EC. A rat model of chronic pressure-induced optic nerve damage. *Exp Eye Res*. 1997;64:85–96.
32. Shareef SR, Garcia-Valenzuela E, Salierno A, Walsh J, Sharma SC. Chronic ocular hypertension following episcleral venous occlusion in rats. *Exp Eye Res*. 1995;61:379–382.
33. Vittitow J, Borrás T. Genes expressed in the human trabecular meshwork during pressure-induced homeostatic response. *J Cell Physiol*. 2004;201:126–137.
34. Olmsted EA, Blum JS, Rill D, et al. Adenovirus-mediated BMP2 expression in human bone marrow stromal cells. *J Cell Biochem*. 2001;82:11–21.
35. Buie LK, Rasmussen CA, Porterfield EC, et al. Self-complementary AAV virus (scAAV) safe and long-term gene transfer in the trabecular meshwork of living rats and monkeys. *Invest Ophthalmol Vis Sci*. 2010;51:236–248.
36. Borrás T, Rowlette LL, Erzurum SC, Epstein DL. Adenoviral reporter gene transfer to the human trabecular meshwork does not alter aqueous humor outflow. Relevance for potential gene therapy of glaucoma. *Gene Ther*. 1999;6:515–524.

37. Spiga MG, Borrás T. Development of a gene therapy virus with a glucocorticoid-inducible MMP1 for the treatment of steroid glaucoma. *Invest Ophthalmol Vis Sci*. 2010;51:3029–3041.
38. Vora GJ, Lin B, Gratwick K, et al. Co-infections of adenovirus species in previously vaccinated patients. *Emerg Infect Dis*. 2006;12:921–930.
39. Kontiola AI, Goldblum D, Mittag T, Danias J. The induction/impact tonometer: a new instrument to measure intraocular pressure in the rat. *Exp Eye Res*. 2001;73:781–785.
40. Danias J, Kontiola AI, Filippopoulos T, Mittag T. Method for the noninvasive measurement of intraocular pressure in mice. *Invest Ophthalmol Vis Sci*. 2003;44:1138–1141.
41. Magne D, Julien M, Vinatier C, Merhi-Soussi F, Weiss P, Guicheux J. Cartilage formation in growth plate and arteries: from physiology to pathology. *Bioessays*. 2005;27:708–716.
42. Mathieu P, Voisine P, Pepin A, Shetty R, Savard N, Dagenais F. Calcification of human valve interstitial cells is dependent on alkaline phosphatase activity. *J Heart Valve Dis*. 2005;14:353–357.
43. Dan H, Simsa-Maziel S, Reich A, Sela-Donenfeld D, Monsonego-Ornan E. The role of matrix gla protein in ossification and recovery of the avian growth plate. *Front Endocrinol (Lausanne)*. 2012;3:79.
44. Cone FE, Steinhart MR, Oglesby EN, Kalesnykas G, Pease ME, Quigley HA. The effects of anesthesia, mouse strain and age on intraocular pressure and an improved murine model of experimental glaucoma. *Exp Eye Res*. 2012;99:27–35.
45. Samsel PA, Kisiswa L, Erichsen JT, Cross SD, Morgan JE. A novel method for the induction of experimental glaucoma using magnetic microspheres. *Invest Ophthalmol Vis Sci*. 2011;52:1671–1675.
46. Borrás T, Gabelt BT, Klintworth GK, Peterson JC, Kaufman PL. Non-invasive observation of repeated adenoviral GFP gene delivery to the anterior segment of the monkey eye in vivo. *J Gene Med*. 2001;3:437–449.
47. Gao X, Usas A, Lu A, et al. BMP2 is superior to BMP4 for promoting human muscle derived-stem cell mediated bone regeneration in a critical size calvarial defect model [published online ahead of print November 1, 2012]. *Cell Transplant*. doi:10.3727/096368912X658854.
48. Zhou L, Li Y, Yue BY. Glucocorticoid effects on extracellular matrix proteins and integrins in bovine trabecular meshwork cells in relation to glaucoma. *Int J Mol Med*. 1998;1:339–346.
49. Silverio KG, Davidson KC, James RG, et al. Wnt/beta-catenin pathway regulates bone morphogenetic protein (BMP2)-mediated differentiation of dental follicle cells. *J Periodontal Res*. 2012;47:309–319.
50. Corr M. Wnt-beta-catenin signaling in the pathogenesis of osteoarthritis. *Nat Clin Pract Rheumatol*. 2008;4:550–556.
51. Chen Y, Whetstone HC, Youn A, et al. Beta-catenin signaling pathway is crucial for bone morphogenetic protein 2 to induce new bone formation. *J Biol Chem*. 2007;282:526–533.
52. Wang WH, McNatt LG, Pang IH, et al. Increased expression of the WNT antagonist sFRP-1 in glaucoma elevates intraocular pressure. *J Clin Invest*. 2008;118:1056–1064.
53. Comes N, Borrás T. Individual molecular response to elevated intraocular pressure in perfused postmortem human eyes. *Physiol Genomics*. 2009;38:205–225.
54. Shen X, Ying H, Yue BY. Wnt activation by wild type and mutant myocilin in cultured human trabecular meshwork cells. *PLoS One*. 2012;7:e44902.
55. Kwon HS, Lee HS, Ji Y, Rubin JS, Tomarev SI. Myocilin is a modulator of Wnt signaling. *Mol Cell Biol*. 2009;29:2139–2154.
56. Shepard AR, Millar JC, Pang IH, Jacobson N, Wang WH, Clark AF. Adenoviral gene transfer of active human transforming growth factor-{beta}2 elevates intraocular pressure and reduces outflow facility in rodent eyes. *Invest Ophthalmol Vis Sci*. 2010;51:2067–2076.
57. Robertson JV, Golesic E, Gauldie J, West-Mays JA. Ocular gene transfer of active TGF-beta induces changes in anterior segment morphology and elevated IOP in rats. *Invest Ophthalmol Vis Sci*. 2010;51:308–318.
58. Junglas B, Kuespert S, Seleem AA, et al. Connective tissue growth factor causes glaucoma by modifying the actin cytoskeleton of the trabecular meshwork. *Am J Pathol*. 2012;180:2386–2403.
59. Borrás T, Gabelt BT, Klintworth GK, Peterson JC, Kaufman PL. Non-invasive observation of repeated adenoviral GFP gene delivery to the anterior segment of the monkey eye in vivo. *J Gene Med*. 2001;3:437–449.

Investigative Ophthalmology & Visual Science